World Journal of Microbiology and Biotechnology (2020) 36:143
https://doi.org/10.1007/s11274-020-02919-x

ORIGINAL PAPER

In vitro and in silico studies on the structural and biochemical insight of anti-biofilm activity of andrograpanin from *Andrographis paniculata* against *Pseudomonas aeruginosa*

Moumita Majumdar[1] · Amit Dubey[2] · Ritobrata Goswami[3] · Tarun Kumar Misra[1] · Dijendra Nath Roy[4]

Received: 12 June 2020 / Accepted: 18 August 2020 / Published online: 27 August 2020

Abstract

Microbial infections have become a global threat to drug-tolerant phenomena due to their biofilm formatting capacity. In many cases, conventional antimicrobial drugs fail to combat the infection, thus necessitating the discovery of some alternative medicine. Over several decades, plant metabolites have played a critical role in treating a broad spectrum of microbial infections due to its low cytotoxicity. Andrograpanin, a secondary metabolite, is a diterpenoid present in the leaf of *Andrographis paniculata.* In this study, andrograpanin (0.15 mM) exhibited significant inhibition on biofilm production by *Pseudomonas aeruginosa* in the presence of gentamicin (0.0084 mM). The impaired production of extracellular polymeric substances and several virulence factors of *Pseudomonas aeruginosa* were investigated to understand the mechanism of action mediated by andrograpanin. The structural alteration of biofilm was evaluated by using fluorescence microscopy, atomic force microscopy and field emission scanning electron microscopy. The in silico molecular simulation studies predicted interaction of andrograpanin with quorum sensing proteins such as RhlI, LasI, LasR, and swarming motility protein BswR of *Pseudomonas aeruginosa*. Overall the studies indicate that andrograpanin could be used as a therapeutic molecule against biofilm development by *Pseudomonas aeruginosa*.

Electronic supplementary material The online version of this article (https://doi.org/10.1007/s11274-020-02919-x) contains supplementary material, which is available to authorized users.

Extended author information available on the last page of the article

Graphic abstract

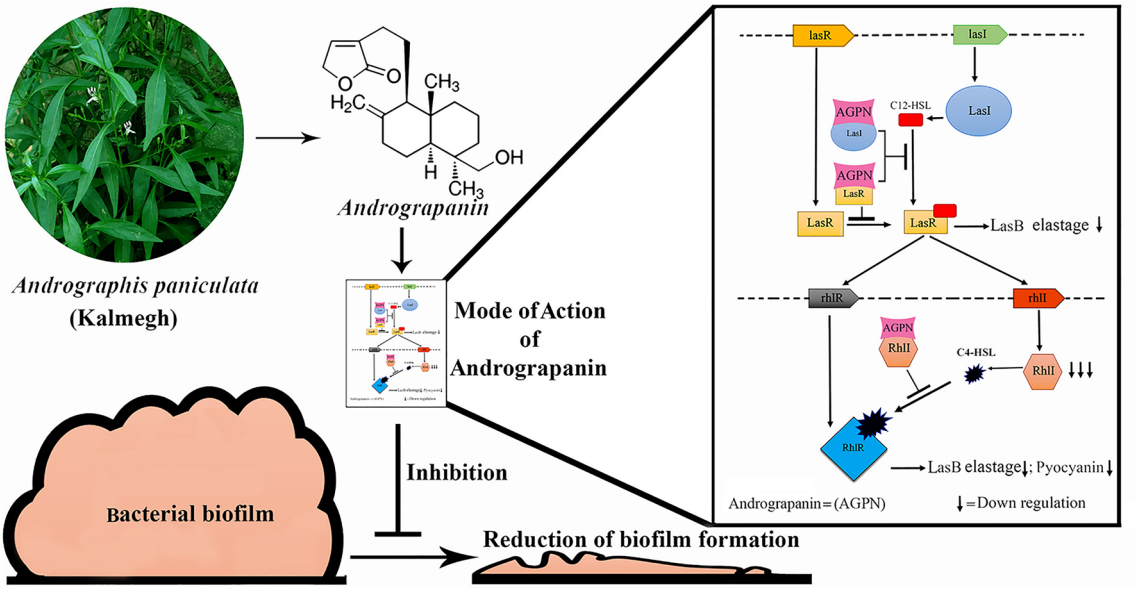

Keywords Andrograpanin · Biofilm · *Pseudomonas aeruginosa* · Quorum sensing inhibitor

Introduction

One of the principal reasons for human mortality is due to nosocomial infection by various infectious agents like viruses, bacteria, parasites, etc. impacting the wellbeing in today's society (Wu et al. 2011; Haque et al. 2018). Bacteria develop tolerance against conventional antibiotics due to excessive and uncontrolled use. Due to this phenomenon, it is almost impossible to eradicate them from the human population. *Pseudomonas aeruginosa*, a Gram-negative bacterium, is one of the model microorganisms for research in the field of medical microbiology, and this bacterium is responsible for approximately 70% of hospital-acquired infections (Wu et al. 2011). *P. aeruginosa* exhibits a strong tolerance towards conventional antibiotic treatment due to biofilm formation in the bacterial colony (Cepas et al. 2019). Biofilm can display drug-tolerance capacity because of the presence of the multilayer structure, which acts as a potential barrier against the host defence and as well as externally added antibiotics. This structure helps the bacteria under biofilm to escape the hostile effect of drugs and make them less susceptible than planktonic cells (Bjarnsholt 2013). Biofilm exhibits the highest tolerance to antibiotics in its fully developed phase (Soto 2013). Additional mechanisms are also involved in the antimicrobial drug resistance and tolerance, including genetic modification, alteration of metabolic status and up-regulation of efflux pumps of the bacteria (Pearson et al. 1999). Biofilm is comprised of cell subpopulations, some of which are metabolically active, and some subpopulations are inactive. These subpopulations show different altered phenotypes against antibiotics as most antibiotics function in metabolically active cells (Pamp et al. 2008). The metabolically inactive cells show less susceptibility to the antibiotics like tetracycline, gentamicin, and chloramphenicol than that of the active cell subpopulation and become tolerant to the conventional antibiotics (Pamp et al. 2008).

Thus, biofilm is an important defence mechanism and a facilitator of bacterial pathogenesis in the host. The formation of biofilm enables the bacterial cell to attach with the surface the living host or the nonliving substratum (Donlan 2002). After reaching a threshold of cell density in a bacterial population, the formation of biofilm is initiated by the secretion of some extracellular polymeric substances such as polysaccharide, proteins, lipids and extracellular DNAs (Costa et al. 2018). These biological processes are governed by the major signalling pathway named quorum sensing (QS) (Lu et al., 2005), in which some chemicals are secreted depending on the cell density of accumulated bacteria. These are mainly bacterial pheromones, called auto-inducers (AI-1 and AI-2). The molecules further moderate the downstream gene expressions, which lead to the secretion of proteins that cause expression of bacterial responses such as the production of specific virulence factors including pyocyanin, rhamnolipid, elastase, protease.

(Moradali et al. 2017; Soni et al., 2008). The quorum sensing of *P. aeruginosa* is controlled by two *N*-acyl-homoserine lactone (AHL)-dependent cell signalling pathways. *las* and *rhl*, are the two principle genes regulating the expression of N-3-oxododecanoyl-L-homoserine lactone (3-oxo-C12-HSL) and *N*-butanoyl-L-homoserine lactone (C4-HSL), respectively following a hierarchy. These two autoinducer molecules act as transcriptional activators modulating the expression of virulence factors responsible for biofilm mediated pathogenesis (Diggle et al. 2002; Medina et al. 2003; Mukherjee et al. 2017).

An alternative new therapeutic approach to treat biofilm-associated antibiotic-tolerant bacteria like *P. aeruginosa* is bioactive plant-based products (Choudhury et al. 2016; Das et al. 2016; Abinaya and Gayathri 2019; Ghosh et al. 2019; Majumdar and Roy 2019; Majumdar et al. 2020). These are mainly secondary metabolites of plants, which effectively constrain the formation of biofilm by limiting the number of bacteria but also inhibit the production of signalling molecules of QS system (Gao et al. 2003; Simoes et al. 2009; Cragg and Newman 2013). *Andrographis paniculata* is a well-known plant that is used as a potential herbal medicine all over the world, especially in many countries of Asia Pacific (Singha et al. 2003; Banerjee et al. 2017). Due to the presence of diterpenoids, flavonoids, and polyphenols, the plant extract has been used to treat anti-inflammatory, anti-parasitic, and antibacterial infections from decades (Li et al. 2006; Roy et al. 2010, 2011; Ooi et al. 2011; Roy et al. 2011; Ma et al. 2012; Majumdar, Biswas et al. 2019). Many research groups have reported that antibiofilm activity of the extract of *A. paniculata* against *P. aeruginosa* (Donlan and Costerton 2002; Ooi et al. 2011; Barsoumian et al. 2015). One of the important bioactive compounds present in the extract is andrograpanin (AGPN) (Liu et al. 2008), which is a hydrolyzed product of another major compound named neoandrographolide of *A. paniculata* (Liu et al. 2008). Many therapeutic applications of andrograpanin have been reported in recent years. Importantly, andrograpanin also has an inhibitory role in HIV infection (Niranjan Reddy et al. 2005).

In this study, we report the efficiency of andrograpanin against biofilm formation by *P. aeruginosa*. It is observed that AGPN potentially inhibits biofilm formation, substantiated by several experiments on biochemical, physical and computational aspects. The inhibitory action of AGPN demonstrates the synergistic effect in the presence of standard antibiotic gentamicin against biofilm development along with suppression of some important virulence factors production. Assessment through molecular docking predicts the binding affinity of AGPN to several proteins related to biofilm production, which might play a role in reducing biofilm production. These findings suggest AGPN could be used as a promising antibiofilm agent.

Materials and methods

Reagents

Andrograpanin (Sigma-Aldrich, USA; Cat. No. 19,443), Tryptone Soya Broth (HiMedia), Safranin (HiMedia), Congo Red (HiMedia), Azocasein (HiMedia) Nutrient Agar (HiMedia), Glucose (HiMedia), Glutaraldehyde (Loba-Chemie), Osmium tetroxide (Loba-Chemie) and all other required chemicals were purchased from reputed companies.

Microbial cultivation

Pseudomonas aeruginosa wild-type (strain number: MTCC 7814) was used in this study. This strain available in North-East of India was isolated and deposited by Dr. B.K. Kanwar, (Department of Molecular Biology & Biotechnology, Tezpur University, India). This strain was previously used for the antimicrobial study (Roy et al. 2013; Majumdar et al. 2019a, b, 2020) Similar to our previous studies, the bacteria were primarily cultured on Tryptone Soya Agar (TSA) plate. A single colony of *P. aeruginosa* was isolated from the TSA plate by a single colony isolation method and incubated in Tryptone Soya Broth (pH 7.4) at 37 °C for 24 h. 10^6 CFU/mL cell suspension of mid-log phase was prepared from this overnight culture for all following investigations on biofilm study (Debnath et al. 2020).

Development and estimation of biofilm growth

For the development of biofilm by *P. aeruginosa*, sterile 96-well plates (polypropylene tissue culture plates, flat-bottom) were used. Primarily, 10^6 CFU/mL cell suspension was added in each well of 96-well plate comprising of 200 µL of TSB media and incubated at 37 °C for 48 h. After incubation, the cultures of each well was discarded, rinsed with sterilized distilled water for three times and kept for air dry. The attached biofilm of each well was stained with safranin 0.5% (w/v) for and incubated for 10 min. Excess stain was rinsed out with 0.9% saline, and the 96-well plate was kept to become completely dry. Adherent biofilms with stain dissolved in glacial acetic acid (30%, w/v). The absorbance was measured at 492 nm using a microplate reader (Diatek LWR96, Kolkata India) (Majumdar et al. 2019a, b).

Determination of minimum inhibitory concentration (MIC)

The minimum inhibitory concentration (MIC) of gentamicin and andrograpanin was determined by using the

broth microdilution method as per Clinical and Laboratory Standards Institute (CLSI) for this study (Patel 2017).

Determination of bacterial growth

The cell suspension of *P. aeruginosa* (10^6 CFU/mL) was incubated at 37 °C for 24 h in TSB media supplemented with sub-MICs doses of AGPN and GEN. The assay was performed by using a sub-MIC dose of AGPN and GEN separately in the wells, as well as in a combination of sub-MIC doses of both in a single well in sterile 96-well plates. The absorbance of bacterial growth was recorded at every 4 h interval upto 24 h at 595 nm using a microplate reader (Diatek LWR96) (Wallis et al. 1981).

Evaluation of the anti-biofilm activity of andrograpanin

This experiment was designed to determine the anti-biofilm action of andrograpanin individually or in combination with the sub-MIC dose of gentamicin (GEN) (0.0084 mM). The bacterial cell suspension (10^6 CFU/mL) was incubated for 48 h at 37 °C with andrograpanin and combination with GEN. Estimation of biofilm growth under the exposure of the drug of interest was evaluated at 492 nm following standard methods, as earlier mentioned (Schillaci et al. 2013; Das et al. 2016). The percentage of biofilm inhibition was calculated of all experimental sets with respect to untreated control.

Assessment of total exopolysaccharide of biofilm

The assessment of the total polysaccharide content of biofilm was determined by the phenol-sulphuric acid method. A combination of 1 mL of freshly prepared 5% phenol and 5 mL of 96% sulphuric acid was mixed with 200 µL of the biofilm sample, as previously mentioned at 30 °C for 15 min. The optical density (O.D) was measured at 490 nm (Combrouse et al. 2013).

Assessment of total protein of biofilm

The total protein of biofilm made by *P. aeruginosa* was determined by the Bradford protein estimation method. Concisely, 10^6 CFU/mL cell suspension was incubated with a different dose of andrograpanin (0.125 mM, 0.15 mM) with a combination of the sub-MIC dose of GEN at 37 °C for 48 h. Here the untreated set was considered as control. After discarding the planktonic cells, adhered biofilm was gently rinsed with sterile PBS (pH 7.1). The content of each well was sonicated at 50 Hz for 45 min, followed by protein estimation test by Bradford reagent, and O.D was measured at 595 nm (Combrouse et al. 2013; Majumdar et al. 2019a).

Assessment of extracellular free deoxyribonucleic acid (eDNA)

Estimation of extracellular DNA (eDNA) was performed after treatment with andrograpanin and gentamicin by UV spectrophotometer by recording the absorbance at 260 nm after DNA extraction from biofilm with bacterial genomic DNA purification kit following manufacturer's instructions (Majumdar et al. 2019a).

Assessment of interactions between antimicrobial compounds

The interaction of AGPN with GEN was determined by checkerboard titration method using a 96-well plate. A series of fractional (1/2, 1/4, 1/8) concentrations of the MIC value of both the compounds were assayed to understand the interactions between them. The following equation calculated the Fractional Inhibitory Concentration (FIC) Index for combinations of AGPN and GEN against *P. aeruginosa*:

$$FIC_{Index} = FIC_A + FIC_B = A/MIC_A + B/MIC_B,$$

where A is the MIC of compound A (AGPN), and B is the MIC of compound B (GEN), considered during combined treatment. MIC_A represents the MIC of compound A (AGPN), and MIC_B represents the MIC of compound B (GEN). The interaction is determined based on the FIC index, where FIC Index ≤ 0.5 represents synergistic effect; > 0.5 to ≤ 1 represents additive effect and FIC index > 1 indicates antagonistic interaction (Eliopoulos and Moellering Jr 1996).

Identification of biofilm by fluorescence microscopic study

An inverted fluorescence microscope was used to assess the andrograpanin treated and untreated biofilm of *P. aeruginosa.* After 48 h incubation with the drug, treated and untreated samples were stained with Congo Red for 20 min in the dark to determine the polysaccharide content present in biofilm through microscopy. Excess stain was washed with PBS (pH 7.2) for two times. The coverslip containing biofilm was seen under the fluorescence microscope (Zeiss AXIO observer, Oberkochen, Germany) with Congo red stain (Jung et al. 2015).

Studies of biofilm topography by atomic force microscopy (AFM)

AFM analysis of biofilm was carried out on the mica sheet with minor modifications from earlier reports (Hu et al.

2012; Majumdar et al. 2019a). The treated and untreated groups of samples fixed on the mica sheet containing biofilms were analyzed, and the images were captured by the microscope (Bruker Multimode 8, MA, USA). The roughness of biofilm was evaluated with NanoScope Analysis v1.40 software.

Estimation of exoprotease activity

The following methodology evaluated the exoprotease activity of *P. aeruginosa*. 48 h treated and untreated cultures were spun down at 10,000 rpm for 5 min. 150 µL of the supernatant of each experimental set was incubated with 1 mL of azocasein (0.3% in 0.05 m Tris–HCl, pH 7.5) for 15 min at 37 °C following the addition of 0.5 mL of trichloroacetic acid (10%) to the reaction mixture, and centrifuged at 10,000 rpm for 5 min. The absorbance of the supernatant was measured at 400 nm (Kessler and Safrin 1994). Here the increased absorbance indicates the presence of protease in the sample, which can digest azoprotein and release the azo dye. Absorbance is directly proportional to the protease present in the sample.

Determination of LasB activity

Elastin Congo red (ECR) assay was performed to estimate the elastase activity of *P. aeruginosa.* Briefly, 50 µL of culture supernatant was added to ECR (10 mg/mL in 0.1 m Tris–HCL, pH 7.0). The absorbance of the centrifuged sample was measured at 495 nm after 17 h incubation at 37 °C under shaking condition (Toder et al. 1991). Elastin digestion by elastase allows the dye to release from the dye–elastin complex. The increasing rate of absorbance is directly proportional to the amount of enzyme present in the sample.

Estimation of the rhamnolipid production

Estimation of rhamnolipid production by *P. aeruginosa* was performed by the orcinol method (Gutierrez et al. 2013). Initially, 500 µl of culture supernatant of treated and untreated groups were extracted two times with 1.5 mL of diethyl ether and centrifuged at 10,000 rpm for 5 min at 4 °C. The pellets were air-dried and re-suspended in 100 µL of double-distilled water. 800 µL of 60% (v/v) sulphuric acid with 100 µL of 1.7% orcinol solution was mixed with the subsequent solution of interest. The absorbance was recorded at 420 nm after heating the solution at 80 °C for 30 min in a water bath. The percentage of production of rhamnolipid was calculated with respect to the untreated group. Rhamnolipids are converted into methyl furfural through hydrolysis and thus reacts with orcinol, which leads to the formation of a blue-green colour solution, which is measured at 420 nm.

Estimation of pyocyanin

The investigation of pyocyanin production was performed by the well-known method established by Essar et al. The cell suspension 10^6 CFU/mL of *P. aeruginosa* was incubated as designed experimental sets with andrograpanin and gentamicin for 48 h at 37 °C. The supernatants were collected after centrifugation at 10,000 rpm for 5 min. Consequently, 3 mL of chloroform was mixed with 5 mL of supernatant and extracted using 0.2 N HCl. The solutions were changed to orange-pink colour, and absorbance was measured at 520 nm (Majumdar et al. 2019a).

Measurement of swarming motility of *Pseudomonas aeruginosa*

To determine the swarming motility movement of *P. aeruginosa*, nutrient agar (8 g/L) supplemented with glucose (5 g/L) was considered as a media for conducting experiments. The polystyrene plates containing media were incubated with cell suspensions of 48 h treated and the untreated group of *P. aeruginosa* culture at the centre of the plates. The plates were incubated for 48 h at 37 °C, and spreading distance due to bacterial growth from inoculation point was measured (Das et al. 2016).

Molecular docking simulation

Molecular simulation studies investigated the binding efficiency of AGPN [ligand, Pubchem Id: 11,666,871 (Kim et al. 2015)] into the active sites of four proteins, namely RhlI [PDB ID: 1KZF (Watson et al. 2002)]; LasI [PDB ID: 1RO5 (Gould et al. 2004)]; LasR [PDB ID: 3IX3 (Bottomley et al. 2007)]; BswR [PDB ID: 4O8B (Wang et al. 2014)] related with biofilm formation pathways of *Pseudomonas aeruginosa* (MTCC 7814). Two different simulation softwares were used to evaluate the binding activity of AGPN with quorum sensing proteins of *P. aeruginosa* [AutoDock version 4.2.6 for setting up the system with ADT 1.5.6 software (Morris et al. 2009) and Glide release 2015-3 software (Schrodinger LLC, New York, NY, USA) (Repasky et al. 2007)].

According to the AutoDock Lamarckian genetic algorithm, polar hydrogens were added to the proteins and ligands, and charges were assigned according to Gasteiger (Gasteiger and Marsili 1980). Further, after identification of residues present in the active site of each protein, as described in PDB, was used to set up the grid map with a spacing of 0.375 Å and focused on the active sites for docking score calculations. The dimensions of this grid map were set up for each protein accordingly to fit each active site [dimension ($78 \times 60 \times 72$ points for 1KZF; $84 \times 72 \times 94$ points for 1RO5; $56 \times 64 \times 120$ points for 3IX3; $64 \times 98 \times 84$

points for 4O8B with the spacing of 0.375 Å]. Before docking, the water molecules and ligands present in crystallographic structures were removed. For andrograpanin ligand, 100 docking runs were performed, selecting the target protein as rigid along with the ligand as flexible. The maximum number of energy evaluations to 2,500,000 was set, and the remaining parameters were set as default (Dubey et al. 2016). Docking poses were clustered using an RMSD value of 2.0 Å. The best-posed representative conformations for each compound were selected after evaluation. A total of 50 decoy molecules of AGPN have been generated with the help of DUD-E website (http://dude.docking.org/generate) and Glide release 2015-3 software (Schrodinger LLC, New York, NY, USA) (Mysinger et al. 2012) to reinforce the in silico outcomes. Besides, these decoy molecules of AGPN were docked against four proteins, such as LasR; LasI; RhlI and BswR. Besides, based on literature, other ligands that used to bind effectively with each protein of interest were checked further in a similar docking platform to validate our findings (Parai et al. 2018; Qais et al. 2019). Protein Preparation Wizard of Maestro graphical user interface (Schrodinger LLC, New York) was employed for making structure for Glide. Ionization states and tautomeric states were generated along with the addition of Hydrogens by Epik (Shelley et al. 2007), and PROPKA was used for the orientation setting of proteins (Olsson et al. 2011). Standard precision was used to dock all the ligands enabling of post-minimization and addition of penalties of Epik state to docking scores. The maximum of 100 poses was documented for each ligand-protein interactions. After that, the Glide Score and Glide Emodel scores were originated following standard protocols (Dubey et al. 2019). The Emodel was used for pose selection (picks the "best" pose of the ligand) in Glide, and then with the help of the Glide Score, the best poses were ranked. Increased negative values explained a stronger binding affinity.

The results from Autodock and Glide docking were saved as .pdbqt extension and .pdb extensions, respectively. Discovery Studio Visualizer tools were used to analyze the interactions between the ligand and proteins.

Quantitative analysis lasR and rhlI mRNA by qRT-PCR

Pseudomonas aeruginosa MTCC 7814 was treated for 48 h at 37 °C with the sub-MIC dose of andrograpanin in combination with gentamicin. TRIzol Reagent (Invitrogen™, CA, USA) was used for the extraction of total RNA from treated and untreated groups. cDNA from this isolated RNA was synthesized by using the Verso cDNA synthesis kit (Thermo Fisher Scientific, USA) following the manufacturer's instruction. RT-qPCR was performed for the *lasR* and *rhlI* gene with Power Up™ SYBR green master mix (Applied Biosystems, CA, USA) with respective primers (*lasR*-Forward: 5′-ACGCTCAAGTGGAAAATTGG-3′; Reverse: 5′- GTAGATGGACGGTTCCCAGA-3′, *rhlI*-Forward: 5′-CTCTCTGAATCGCTGGAAGG-3′; Reverse: 5′-GACGTCCTTGAGCAGGTAGG-3′). Primary (citable) accession number: A7UJ09 represents *lasR*, the Primary (citable) accession number: P54291 represents *rhlI*. Quantitative RT-PCR (Quant Studio5 Real-Time PCR system, Applied Biosystems) was performed under the following set of temperatures at 50 °C for 2 min and followed by initial denaturation for 10 min at 94 °C. Consecutively, 30 PCR cycles were performed at 94 °C for 20 s and 60 °C for 1 min. 16 s *rRNA* was considered as an endogenous control gene. The fold change was calculated from the critical threshold cycle (C_T) value. The change-in-threshold $2^{(-\Delta\Delta CT)}$ method was used to calculate the relative expression of the treated group compared to the control (untreated) group (Lee et al. 2008).

Structural studies of biofilm by FE-SEM

The field emission scanning electron microscopy (FE-SEM) was performed to evaluate the effect of andrograpanin on the structural aspect of biofilm made by *P. aeruginosa.* The treated and untreated biofilms were developed on 10 mm round coverslips for 48 h followed by 2 h incubation with 2.5% glutaraldehyde (v/v 0.1 PBS, pH 7.3) at 4 °C for fixing the cells. After three consecutive washes with buffer, all coverslips were treated with 1% osmium tetroxide for 1 h at 4 °C followed by dehydration in a series of ethanol (30%, 50%, 70%, 90%, and 100%). Samples were dried enough before SEM analysis. Images of the sample were recorded by FE-SEM (Sigma-300, Carl Zeiss) with 6000× magnification (Priester et al. 2007).

Statistical analysis

Minimum three independent replicate experiments were performed to obtain a statistically significant result. Experimental outcomes were expressed as mean ± standard deviation. The statistical significance of triplicates was calculated by using one-way ANOVA using Turkey's multiple comparisons test with Graph Pad Prism 7.00 software. The p value of 0.05, was considered to mention as statistically significant.

Result

Determination of MIC of AGPN and GEN

The Gram-negative bacterium *Pseudomonas aeruginosa* (MTCC 7814) is an established model organism for biofilm research. Initially, we estimated the MIC value of AGPN and

GEN before conducting any anti-biofilm study using those molecules. The objective is to calculate the MIC value of AGPN and GEN to understand the toxicity of AGPN against Pseudomonas bacteria. As we know, if a bacterium is sick or dying, it cannot make biofilm or any other virulence factor. Accordingly, the minimum inhibitory concentration (MIC) of AGPN and Gentamicin (GEN) was determined at 0.832 mM and 0.021 mM, respectively.

AGPN inhibits biofilm formation

The bacteria *Pseudomonas aeruginosa* (MTCC 7814) showed significant attenuation of biofilm production due to exposure to AGPN in a dose-dependent manner. The compound's effect was evaluated in its sub-MIC dose, which was further increased by the addition of the sub-MIC dose of GEN to the experimental set. AGPN blocked approximately 54% biofilm production at 0.125 mM, which was further augmented by up to 60% at 0.15 mM (Fig. 1a). The sub-MIC dose of GEN (0.0084 mM) has a minor inhibitory effect (~ 10%) on biofilm production. However, the outcome was dramatically changed when the bacteria were treated in combination with AGPN and GEN, as it showed ~ 90% inhibition ($p < 0.0001$) (Fig. 1b). From this observation, this can be stated that a combination of AGPN with GEN has an impact on organisms to inhibit biofilm production, which will be investigated further by conducting the following experiments.

AGPN attenuates EPS production of biofilm

EPS made of polysaccharide, protein, and eDNA are the main constituents of biofilm. To determine the role of AGPN on EPS production of biofilm by *P. aeruginosa*, levels of biofilm carbohydrate, protein and eDNA were estimated. AGPN alone significantly inhibited the extracellular carbohydrate, protein and eDNA production up to ~ 60% at 0.15 mM. This inhibition was further increased up to ~ 91% ($p < 0.0001$) during combined treatment with the sub-MIC dose of GEN (Fig. 1c).

Synergistic effect of AGPN with GEN and their role on bacterial cell viability

From the cell viability assay, no significant change was observed in bacterial cell growth during 24 h treatment with AGPN, sub-MIC dose of GEN, or their combination (Fig. 1d), which confirms the antibiofilm activity of AGPN against *P. aeruginosa* without hampering the cell population. The synergistic interaction of AGPN and GEN was established by the determination of the FIC index at 0.375, thereby reinforcing the effects of antibiofilm activity. Based on previous studies, 0.15 mM of AGPN has been considered for all subsequent experiments, and this amount of dose is quite low compared to the MIC value of AGPN.

Observation of altered biofilm structure through microscopy

In the following experiments, we investigated the structural alteration of biofilm using fluorescence microscopy and atomic force microscopy.

In Fig. 2a, we performed fluorescence microscopy study to observe the stain on the outer surface texture of exopolysaccharide with Congo Red dye. This result clearly illustrates that the maximum red fluorescence was observed in the control group (Control). Still, there was an absence of red fluorescence in the combined drug-treated group (AGPN + GEN). This finding indicates the disruption of multilayer polysaccharide structure due to the presence of AGPN.

The structural details, especially roughness parameters of biofilm, were verified through atomic force microscopy (Fig. 2b). After 48 h treatment of AGPN with the sub-MIC dose of GEN, a significant decrease in roughness was observed up to 34.85 nm in treated groups compared to the control group (462 nm).

Inhibitory effect of AGPN on virulence factors production and swarming motility

To understand the underlying mechanism of biofilm attenuation of *P. aeruginosa* by AGPN alone or in combination with GEN, we have examined the effect of AGPN on QS mediated swarming motility, exoprotease activity, secretion of virulent factors such as rhamnolipid, pyocyanin, and LasB elastase activity.

One of the essential virulence factors, the exoprotease activity, was reduced up to ~ 85% during the combined treatment of AGPN (0.15 mM) with the sub-MIC dose of GEN ($p < 0.0001$) (Fig. 3a). Interestingly, other virulence factors, including LasB elastolytic activity was inhibited up to ~ 87% ($p < 0.0001$) (Fig. 3b), rhamnolipid production was reduced up to ~ 91% ($p < 0.0001$) (Fig. 3c) and pyocyanin production was also quenched up to ~ 93% ($p < 0.0001$) (Fig. 3d) in combined treatment of AGPN (0.15 mM) with a sub-MIC dose of GEN.

Bacterial translocation takes place through an instantaneous movement of well-organized multiple colonies on a substratum through swarming motility (Kumar et al. 2013). *P. aeruginosa* treated with AGPN with sub-MIC GEN showed very little translocation in comparison with untreated control. However, AGPN showed substantial inhibition on the motility movement compared to the antibiotic GEN alone (Fig. 3e).

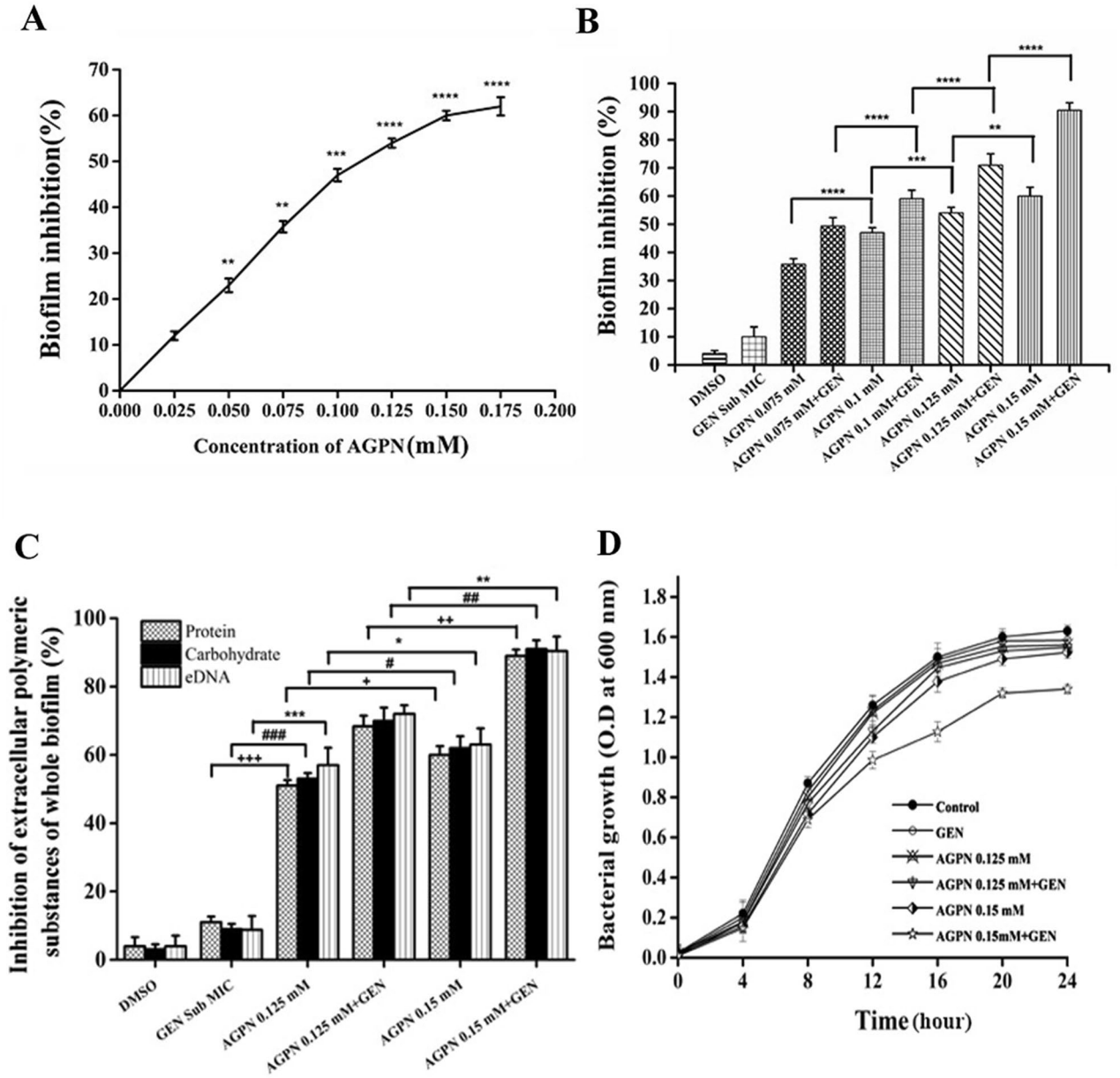

Fig. 1 Studies on dose optimization of AGPN with GEN to inhibit the production of biofilm of *P. aeruginosa*: **a** To optimize the effective concentration of AGPN, a range from 0.025 mM to 0.175 mM were used for this study. The percentage of biofilm inhibition was estimated compared to the untreated control group. **b** Optimization of the effective dose of AGPN (0.075 mM to 0.15 mM) in the presence of GEN (Sub-MIC) on biofilm inhibition. **c** Inhibition of polysaccharide, protein and eDNA of biofilm was estimated using AGPN (0.125 mM to 0.15 mM) in the presence of GEN (Sub-MIC). (#) represents carbohydrate, (*) represents the significance of protein, and (+) represents the eDNA significance. **d** Estimation of effect of AGPN (0.125 mM to 0.15 mM) and GEN (0.0084 mM) on viability of bacterial cells. Experiments were performed in six sets independently. Each value presented as mean ± S.D of the six independent experimental sets. ****$p < 0.0001$; ***$p < 0.001$; **$p < 0.01$; *$p < 0.05$ and *NS* non-significant change. Significance was calculated in comparison with factor 1 (with and without gentamicin), and factor 2 (low and high dose of AGPN) treated groups as well, as indicated in the figure

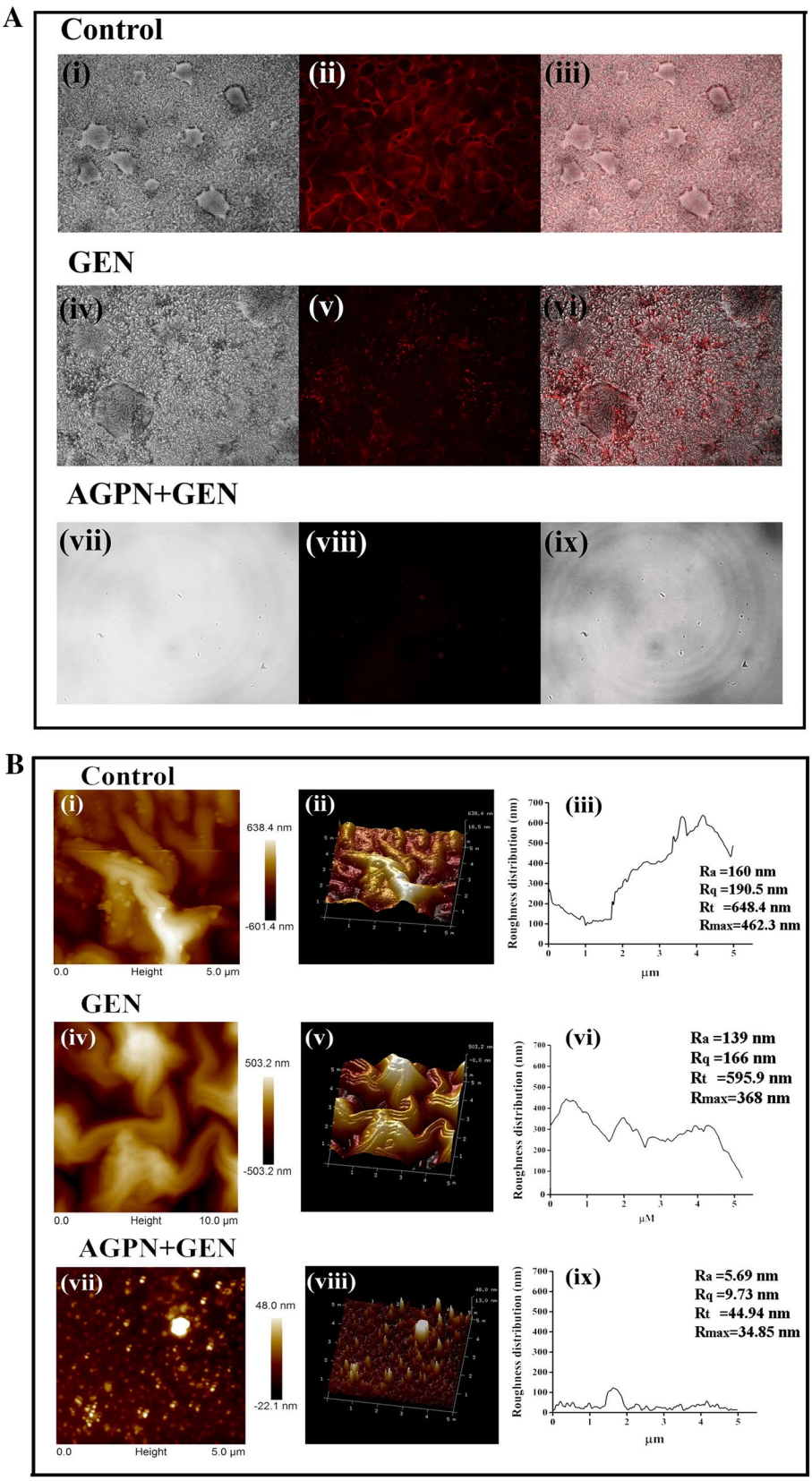

Fig. 2 Studies of biofilm using microscopy: **a** Images i, ii, iii represent control biofilm stained with Congo Red. Images iv, v, vi represent the status of biofilm after treatment with GEN (Sub-MIC, 0.0084 mM) for 48 h. Images vii, viii, ix demonstrate synergistic effects of AGPN (0.15 mM) with GEN (sub-MIC, 0.0084 mM) on biofilm production. The magnification of the photomicrograph is 40×. **b** Images i, ii, iii represent control biofilm indicating two and three-dimensional structures along with roughness distribution. Images iv, v, vi show the effect of GEN (sub-MIC, 0.0084 mM) on biofilm after 48 h treatment. Similarly, images vii, viii, ix present roughness inhibition after exposure in combined treatment of AGPN (0.15 mM) with GEN (sub-MIC, 0.0084 mM). Each image is a representation of six independent experiments

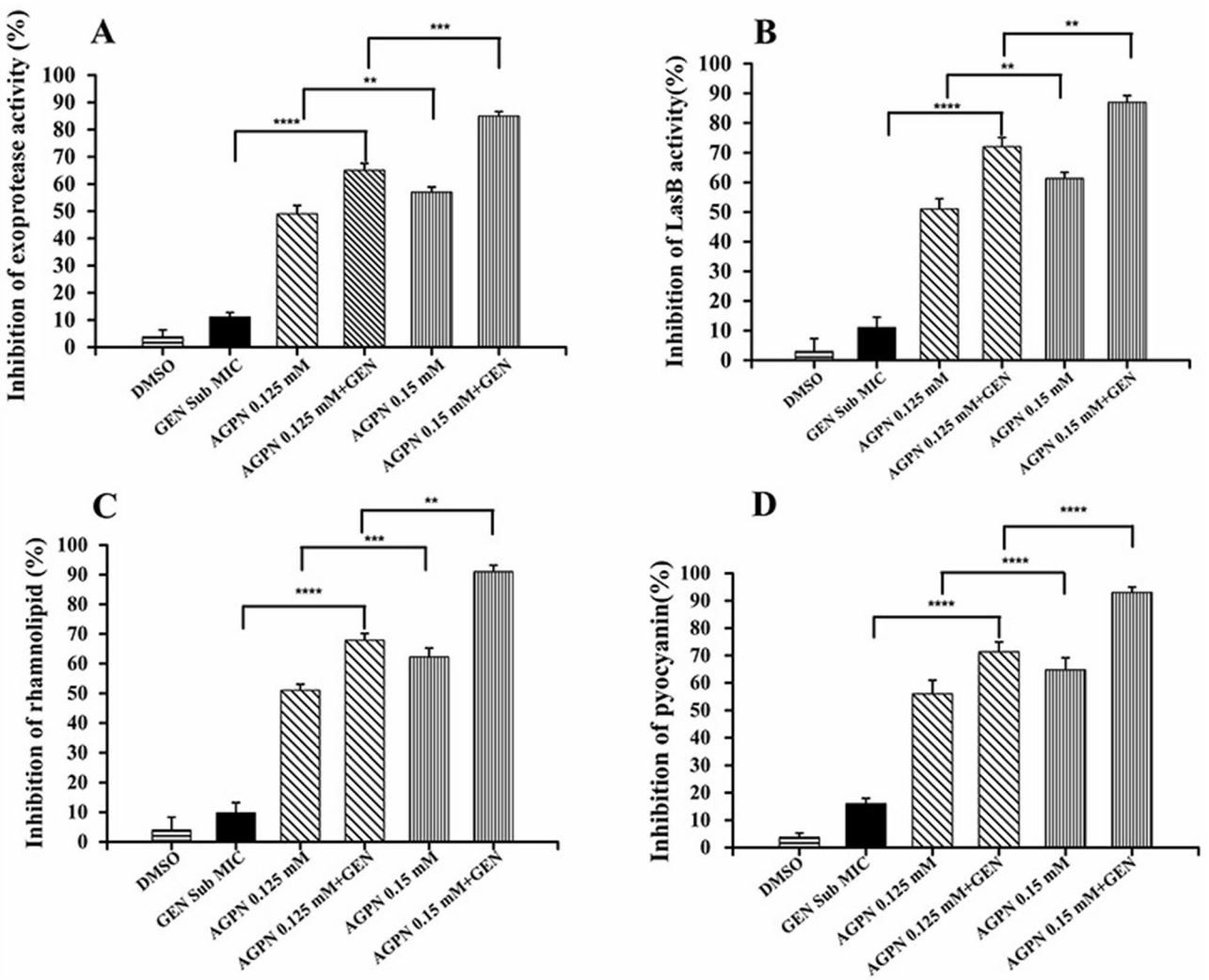
A
Inhibition of exoprotease activity (%)
B
Inhibition of LasB activity(%)
C
Inhibition of rhamnolipid (%)
D
Inhibition of pyocyanin(%)
DMSO
GEN Sub MIC
AGPN 0.125 mM
AGPN 0.125 mM+GEN
AGPN 0.15 mM
AGPN 0.15 mM+GEN

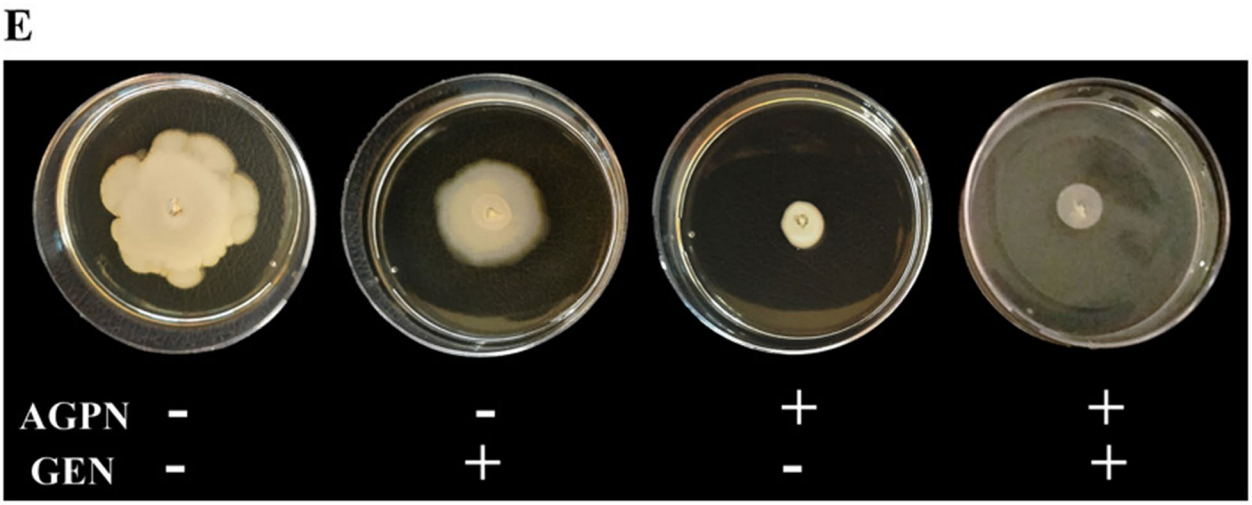
E
AGPN - - + +
GEN - + - +

◂**Fig. 3** The effect of AGPN on the production of virulence factors and the swarming motility of *P. aeruginosa*: The following virulence factors were estimated after AGPN (0.125 mM to 0.15 mM) with GEN (sub-MIC, 0.0084 mM) treatment for 48 h. **a** Percentage of inhibition of exoprotease activity; **b** percentage of inhibition of LasB activity; **c** percentage of inhibition of rhamnolipid production; **d** percentage of inhibition of pyocyanin production. The percentage of inhibition was calculated with respect to control, and each value presented as mean ± S.D of six independent experimental sets. ****$p < 0.0001$; ***$p < 0.001$; **$p < 0.01$; *$p < 0.05$ and *NS* non-significant change. Significance was calculated in comparison with control and among different treated groups as well, as indicated in the figure. **e** The effect of AGPN (0.15 mM) and GEN (sub-MIC, 0.0084 mM) on swarming motility of *P. aeruginosa.* Each image is the representation of three independent experiments

Mechanism of inhibition of quorum sensing (QS) regulator proteins of *P. aeruginosa* by docking studies

Molecular docking was performed to predict the possible binding of AGPN with the protein molecules, including transcription factors, principally involved in the quorum-sensing pathway as well as biofilm formation. The previous experimental outcomes strongly suggested that AGPN inhibited the contribution of quorum sensing factors in biofilm formation. Accordingly, the binding affinity of AGPN was determined towards the active sites of selected four proteins of *P. aeruginosa.* Crystal structures of quorum sensing factors, namely LasI (PDB Code: 1RO5, AHL Synthase), LasR (PDB Code: 3IX3, LasR-OC12 HSL complex), RhlI (PDB Code: 1KZF, acyl-homoserine lactone synthase) and swarming motility protein BswR (PDB Code: 4O8B, transcriptional regulator) were considered for this study. The non-covalent interactions between AGPN and amino acids of proteins are mainly pi-alkyl, alkyl, carbon-hydrogen and hydrogen bonds (Fig. 4) and detailed interactions for binding between AGPN with proteins are listed in Table 1. Glide Software and Autodock Software, both were used to establish the reliability of the binding predictions, and their outcomes were compared (Table 1). Among 50 decoy molecules, the lowest scoring decoy has been considered as the negative control for each of the four proteins. Besides, ligands of these proteins (Parai et al. 2018; Qais et al. 2019) were considered as positive controls, as mentioned in supplementary Table S1. We found that reported positive ligands displayed similar or less binding scores compared to AGPN in a similar docking platform, indicating the possibility of actual binding, thus substantiating the experimental findings. No such ligand has been reported in the literature to date for BswR. Interactions of AGPN, positive control and decoys with four proteins have been illustrated in Supplementary Figure S2 (S2.1 to S2.5). A correlation chart of Glide and Autodock score has been represented in Table S1 and Figure S1.

Docking between AGPN and RhlI

The binding studies between AGPN and RhlI represent the Glide score − 4.956 kcal/mol for the predicted binding (Table 1). In the complex, Ser98 and Ser99 of the active site of the protein interact with AGPN via hydrogen bond and carbon–hydrogen bond, respectively. Further, Phe101 and Met146 are involved in strong pi-alkyl interaction, while Val142 forms an alkyl bond with the ligand.

According to the best-fitted model using Autodock, the predicted binding energy between AGPN and RhlI is − 9.30 kcal/mol (Fig. 4a; Table 1). The representative conformation of the ligand–receptor complex shows AGPN interacts with the residue Arg100 of the active site making a strong alkyl bond. Besides, Tyr54 interacts through strong conventional hydrogen bonds along with the formation of pi-alkyl, pi-sigma while Val67 makes only conventional hydrogen bonds with AGPN.

Docking between AGPN and LasI

The binding studies between AGPN and LasI represent the Glide score − 2.988 kcal/mol for the expected binding (Table 1). In the complex, Arg30 and Thr144 of the active sites interact with AGPN by forming a hydrogen bond and carbon-hydrogen bond, respectively. Phe105 and Phe117 involve in strong pi-alkyl interaction, whereas Val148 participates in alkyl bond formation with AGPN.

According to the predicted binding energy, the value − 8.63 kcal/mol indicates the best-ranked complex among all fitted models (Fig. 4b; Table 1). AGPN interacts with active site residues of LasI protein via the formation of stable hydrogen with Arg30, the alkyl and pi-alkyl bond with Phe105, a pi-alkyl bond with Phe117, and two strong alkyl bonds with Val148.

Docking between AGPN and LasR

As LasR is a dimeric protein containing two identical chains, the binding study between AGPN and LasR protein was performed separately for both the chains. Binding studies between AGPN and LasR (Chain A) represent the Glide score of − 2.702 kcal/mol for the best-predicted complex (Table 1). In the complex, Leu84, Pro85, and Phe87 interact with AGPN via alkyl bond. On the other hand, the binding studies between AGPN and LasR (Chain B) represent the Glide score of − 2.099 kcal/mol for the best-fitted model (Table 1). In that complex, Leu148 interacts with AGPN through the pi-alkyl bond formation.

Based on the best-predicted cluster, binding energy − 6.43 kcal/mol represents the best ligand-receptor complex (Fig. 4c (i), Table 1), and it involves AGPN-Leu8

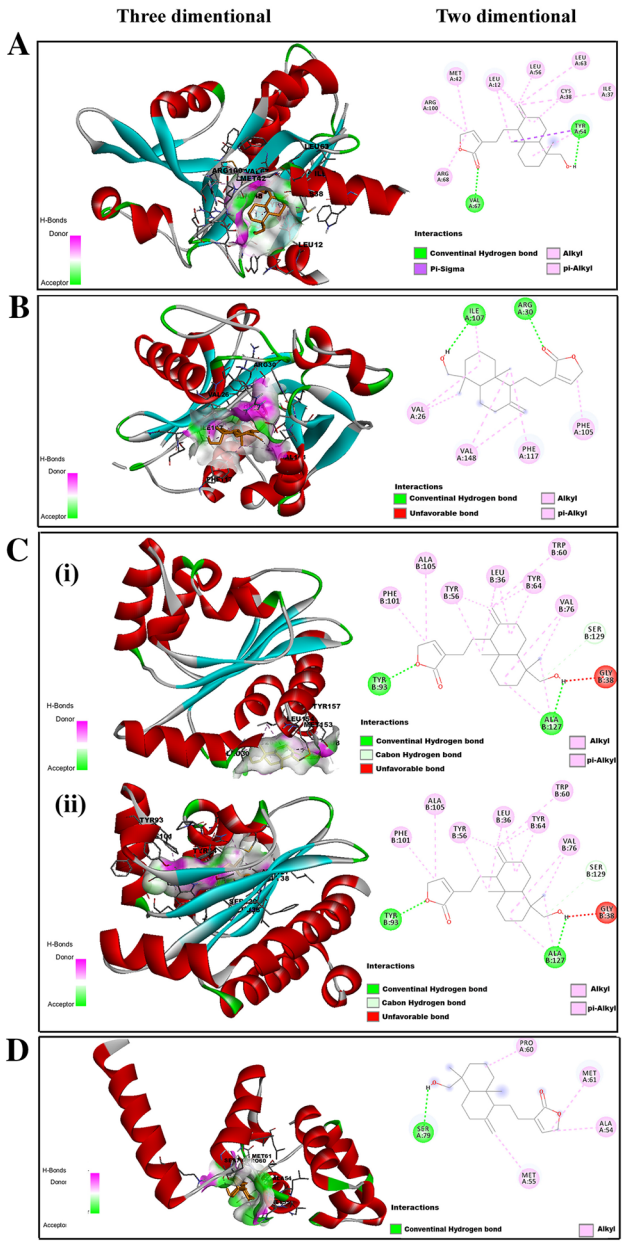

Fig. 4 Molecular docking analyses of possible interactions between AGPN and proteins involved in quorum sensing: the images are in 3D and 2D view generated in Discovery Studio. **a** Images represent the interactions between AGPN and RhlI (PDB ID: 1KZF); **b** images represent the interactions of AGPN with LasI (PDB ID: 1RO5); **c** (i) images represent the interactions between AGPN and LasR chain A (PDB ID: 3XI3), (ii) images represent the interactions of AGPN with LasR chain B (PDB ID: 3XI3); **d** images represent the interactions of AGPN with BswR (PDB ID: 4O8B)

of active site interaction via conventional hydrogen bond. For LasR (Chain B), the predicted binding energy is − 8.22 kcal/mol, which is the best-ranked complex (Fig. 4c (ii), Table 1). The analysis of the representative pose shows that AGPN interacts with Tyr93 by conventional hydrogen bond and with Ala127 through a single hydrogen bond and two alkyl bonds.

Docking between AGPN and BswR

The binding studies between AGPN and swarming motility protein BswR represent the Glide score − 3.798 kcal/mol for the best-predicted binding. In complex, Pro60 and Val78 present in the active site of BswR interact with AGPN through alkyl bond formation (Table 1).

According to the predicted binding energy, Fig. 4d is the best-ranked complex between AGPN and BswR, showing − 6.20 kcal/mol (Table 1). The representative display demonstrates AGPN interacts with Pro60 of protein through alkyl bond formation, similar to the glide docking result.

AGPN declines mRNA expression of lasR and rhlI gene

The real-time PCR of the *lasR* and *rhlI* gene was performed (Fig. 5a) to assess the effect of AGPN on gene regulation in the quorum-sensing pathway. *lasR* is one of the key regulators as it controls both the LasB production and the RhlIR cascade. This *rhlI* gene works as a downstream of signal synthase of *P. aeruginosa*. There was a significant reduction in fold change of the *lasR* and *rhlI* gene expression at mRNA level when treated with AGPN with GEN (0.0723 fold for *lasR* and 0.0394 fold for *rhlI*) compared to the untreated control group.

Alteration of *P. aeruginosa* morphology and its biofilm structure using FE-SEM

All the above experiments further led us to explore the effect of AGPN on *P. aeruginosa* morphology and its biofilm structure using the FE-SEM technique (Fig. 5b). This approach provided us with important information about microscopic structural details, including shape, the size of bacteria, along with the outside texture of biofilm. The control group exhibited the multi-layered dense matrix of EPS, whereas AGPN with GEN reduced the biomass significantly by eradicating the EPS matrix.

Discussion

Microbes become tolerant against antimicrobial drugs through various pathways such as the genetic modification or the formation of a physical barrier called biofilm. The bacteria inside the biofilm are more tolerant than planktonic cells as the drug fails to invade the multi-layered structure of biofilm (Donlan 2002; Saini et al. 2011). This protective shield

Table 1 Molecular docking analysis of andrograpanin (AGPN) with proteins of *P.aeruginosa*

Protein (PDB ID)	Active site residues	Results of docking by Glide software			Results of docking by Autodock software		
		Glide score (kcal/mol)	**Emodel**	**Interactions**	**Best-predicted binding energy (kcal/mol)**	**No. of poses in the cluster with best-predicted energy**	**Interactions**
RhlI (1KZF)	Glu97, **Ser98, Ser99**, **Arg100**, **Phe101**, Val103, Lys105, Ile118, Ser119, Phe123, Met126, Thr140, Ile141, **Val142**, **Met146**, Trp155, Leu176	− 4.956	− 33.493	**Ser98 (conventional hydrogen bond), Ser99 (carbon hydrogen bond)**, **Phe101(pi-alkyl)**, **Val142 (alkyl)**, **Met146 (pi-alkyl)**, Leu150 (alkyl)	− 9.30	4	Leu12 (pi-alkyl), Ile37 (alkyl), Cys38 (pi-alkyl), Met42 (pi-alkyl), Tyr54 (conventional hydrogen bond pi-alkyl, pi-sigma), Leu56 (alkyl), Leu63 (alkyl), Val67 (conventional hydrogen bond), Arg68 (alkyl), **Arg100 (alkyl)**
LasI (1RO5)	Arg23, Phe27, **Arg30**, Ile33, Glu42, Asp44, Asp47, Trp69, Arg70, Phe84, Glu101, Ser103, Arg104, **Phe105**, Met125, **Thr144**, Met151, Met152, Ala155, Leu157, Leu188	− 2.988	− 26.358	**Arg30 (conventional hydrogen bond)**, **Phe117 (pi-alkyl), Phe105 (pi-alkyl), Thr144 (carbon hydrogen bond), Val148 (alkyl)**	− 8.63	80	Val26 (two alkyl), **Arg30 (conventional hydrogen bond)**, **Phe105 (alkyl, pi-alkyl)**, Ile107 (conventional hydrogen bond, alkyl), **Phe117 (pi-alkyl)**, **Val148 (two alkyl)**
LasR Chain A (3IX3)	Phe7, **Leu8**, His78, Leu84, **Pro85**, Ile86, **Phe87**, Glu89, Ser91, Ile92, Leu148, Tyr157	− 2.702	− 18.984	**Leu84 (two alkyl), Pro85 (two alkyl)**, **Phe87 (alkyl)**, Trp152 (two pi-alkyl),	− 6.43	37	**Leu8 (conventional hydrogen bond)**, Met26 (conventional hydrogen bond, alkyl, pi-alkyl), Leu30 (alkyl), Met153 (two alkyl), Leu154 (two alkyl), Tyr157 (two pi-alkyl)
LasR Chain B (3IX3)	Phe7, Leu8, His78, Leu84, Pro85, Ile86, Phe87, Glu89, Ser91, Ile92, **Leu148**, Tyr157	− 2.099	− 15.131	**Leu148 (pi-alkyl)**, Pro149 (carbon hydrogen bond), Trp152 (alkyl, pi-alkyl)	− 8.22	1	Leu36 (two pi-alkyl), Gly38 (unfavourable donor-donor), Tyr56 (two pi-alkyl),Trp60 (alkyl),Tyr64 (two pi-alkyl), Val76 (two pi-alkyl), Tyr93 (conventional hydrogen bond), Phe101 (alkyl), Ala105 (alkyl), Ala127 (conventional hydrogen bond, two alkyl), Ser129 (carbon hydrogen bond)
BswR (4O8B)	Ala62, Tyr65, Leu71, Leu74, Lys77, **Val78**, Leu81, Phe85, Glu94, Leu89, Thr90, Phe92, Ile93, Leu97, Ala99, DNA Binding Site: Arg34, Gln37, Arg42, His43, Asn46, Arg48	− 3.798	− 29.771	Gln58 (conventional hydrogen bond), **Pro60 (alkyl)**, Lys86 (conventional hydrogen bond, carbon hydrogen bond), **Val78 (alkyl)**	− 6.20	21	Ala54 (alkyl), Met55 (alkyl), **Pro60 (alkyl)**, Ser79 (conventional hydrogen bond)

Bold letters indicate the biding of ligand andrograpanin with active site residue of respective proteins

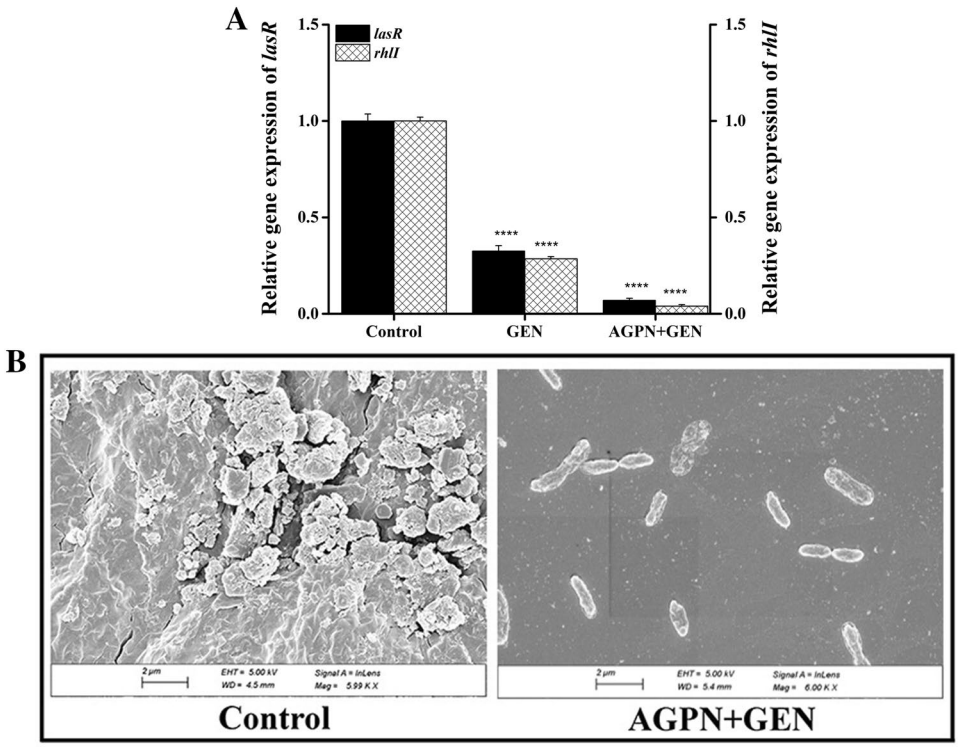

Fig. 5 Effect of combined treatment of AGPN (0.15 mM) with GEN (sub-MIC, 0.0084 mM) on quorum sensing gene regulation and structural change: **a** The result represents the relative expressions of *las R* and *rhlI* after 48 h treatment with AGPN and GEN in comparison with the control group. Each value represents mean ± S.D of the three independent experimental sets. Significance (****$p < 0.0001$) was calculated in respect to control; **b** representative images of FE-SEM show the effect of AGPN with GEN on the structural alteration of biofilm and the distorted cell membrane of *P. aeruginosa*. Each image is the representation of three independent experiments

of bacterial community makes them least susceptible to antibiotics (Lázár et al. 2018; Andersson et al. 2019). In the present study for the very first time, the effect of andrographanin, a diterpene present in the leaf of *A. paniculata* has been evaluated against biofilm formation using model microorganism *P. aeruginosa.* This Gram-negative bacterium is mainly responsible for nosocomial infections in human (Wu et al. 2011). Besides, we evaluated the synergistic effect of the sub-MIC dose of conventional antibiotic gentamicin (GEN) in combination with andrographanin (AGPN) against biofilm developed by *P. aeruginosa* (Fig. 1a and b). The compound AGPN at the level of sub-MIC doses showed significant inhibition of biofilm production, which was further increased by many folds during combined treatment with the sub-MIC dose of GEN, indicating AGPN helps to inhibit biofilm formation. However, the sub-MIC dose of GEN alone was not able to inhibit the production of biofilm, which reflects biofilm had stopped antibiotic penetration towards the microbial cells. This outcome confirmed that AGPN inhibits biofilm formation rather than acting as an antimicrobial agent to kill the bacterial cells as there were no significant differences in the cell viability of bacteria (Fig. 1D). Thus, the applied dose has no cell-killing response towards *P. aeruginosa.*

The biofilm inhibition has a substantial impact on us to investigate further the deep insight of drug action on *P. aeruginosa*. It is well known that biofilm is made of extracellular polymeric substances (EPS) such as extracellular polysaccharides, proteins, and eDNA. Moreover, several signalling molecules are also involved in governing the principle quorum-sensing (QS) pathway, which is responsible for biofilm formation (Medina et al. 2003; Mukherjee et al. 2017). Reduced production of EPS in a dose-dependent manner indicates that AGPN, along with the sub-MIC dose of GEN, potentially blocked the growth of the biofilm matrix (Fig. 1c). This result indicates a reduction of biofilm content, which consists of extracellular matrix and attached cells within the biofilm matrix, excluding planktonic cells. It is assumed that a reduced biofilm matrix enhances the planktonic cell number rather than the number of attached cells with the biofilm, as the total number of cells remained unchanged, as observed in growth curve analysis. Also, the FIC index suggests that the interaction between AGPN and GEN is synergistic rather than additive. In our study, the sub-MIC dose of GEN and AGPN inhibits biofilm production upto 90%, which is indicative of synergistic interaction rather than 70% of additive interaction. The FIC index of 0.375 also substantiates our findings on the interaction between the compounds for biofilm inhibition.

The structural modulation of biofilm was thoroughly investigated using image analysis through a high definition microscope since the quantity of EPS had been reduced after drug treatment. The Congo red is a well-known red fluorescent dye used to stain biofilm because it has a strong and specific binding affinity towards polysaccharides (Kan et al. 2019). In our investigation, the maximum red fluorescence

was observed in the control group. Still, there was no such strong red fluorescence field found in treated groups indicating the inhibition of EPS matrix production by the AGPN and GEN. AGPN (0.15 mM) effectively diminished the EPS production of *P. aeruginosa* (Fig. 2a). The entire topography of one surface can be achieved (Hu et al. 2012) by using atomic force microscopy. In our study, the sharp reduction in height and roughness distribution of biofilm in the AGPN treated samples indicates the inhibitory effect of AGPN on structural parameters of *P. aeruginosa* biofilm. Furthermore, we report that AGPN shows a synergistic effect in reducing the height of biofilm along with the sub-MIC dose of GEN, but it is absent in the group treated with the sub-MIC dose of GEN alone (Fig. 2b). These results further confirmed AGPN is likely the inhibitor of the quorum-sensing pathway.

Pseudomonas aeruginosa contains two QS systems, namely LasI/R and RhlI/R, yield 3-oxo-C12-homoserine lactone (C12-HSL) and C4-homoserine lactone (C4-HSL), respectively (Medina et al. 2003; Mukherjee et al. 2017). The C12-HSL synthesized by the LasI system, which interacts with LasR protein after setting up a critical concentration when the particular microbe achieves a threshold of cell density. On the other hand, the *rhlI* gene plays a crucial role in synthesizing C4-HSL leading to binding with RhlR to activate the transcription of several downstream genes such as *lasB*, *toxA*, and *lasI*. These genes are responsible for the production of a variety of virulence factors such as protease, elastase, rhamnolipid, hydrogen cyanide, pyocyanin, etc. The production of these virulence factors during biofilm formation helps the microbes to get a favourable environment for pathogenesis in the host cells (Moradali et al. 2017). Accordingly, in our approach, assessment of virulence factors production after drug treatment was crucial to get a clear idea about the AGPN action on the quorum-sensing pathway. In our experiments, the antagonistic action of AGPN on the production of virulence factors such as exoprotease, LasB Elastase, rhamnolipid, pyocyanin was assessed (Fig. 3a–d). AGPN at 0.15 mM (sub-MIC) significantly inhibited ($p < 0.001$) those virulence factors generated by *P. aeruginosa*, indicating virulence factors were not synthesized through quorum sensing pathway. Our result is also justified by several other research reports demonstrating anti-biofilm drug action *P. aeruginosa* (Li et al. 2006; Das et al. 2016). In the initial phase of biofilm formation and its attachment to a new substratum by the bacteria using a special flagellar movement termed as swarming motility, which is also present in *P. aeruginosa* (Kearns 2010). In our findings, the antibiotic GEN is not able to stop the flagellar movement of *P. aeruginosa* at sub-MIC dose, but after the addition of AGPN in the similar experimental setup, a combination of these two synergistically stop the flagellar movement including the fact that AGPN alone also significantly stopped the swarming motility (Fig. 3e). This outcome deciphers the inhibitory role of AGPN on swarming motility as well as on the signalling cascade of the quorum-sensing pathway.

The in silico molecular docking study was performed to predict the possible bindings of AGPN with biofilm-associated proteins (RhlI, LasI, LasR, and BswR) of *P. aeruginosa* to understand the probable competitive binding as well as a possible conformational alteration of respective proteins. Already it is established C12-HSL and C4-HSL bind with LasR and RhlI, respectively (Medina et al. 2003; Mukherjee et al. 2017) and C12-HSL, C4-HSl and AGPN, all three have a common lactone moiety in their chemical structures. Analytical data of molecular simulation studies performed in two different platforms (Autodock and Glide) are strongly matched, suggesting that AGPN could effectively interact with active sites residues Ser98, Ser99, Arg100, Phe101 of RhlI and Leu8, Pro85, and Phe87 of LasR (Table 1). This observation suggests that AGPN could replace the autoinducer C4-HSL and C12-HSL from the binding with RhlI and LasR, respectively. The binding of AGPN with the active sites of LasR with a stable hydrogen bond along with alkyl interactions indicates AGPN could act as an agent in the competitive binding phenomenon. This event is also involved similarly during the binding of C4-HSL with RhlI, and finally, the complexes are likely to be considered as AGPN-RhlI and AGPN-LasR (Fig. 4a and c). AGPN effectively binds with the active sites of LasI (Phe105, Thr142, Thr144, and Val148) suggested that it could inhibit the synthesis of AHL synthesis in *P. aeruginosa* (Maisuria et al. 2016). Sideways with QS proteins, in silico studies were performed to predict the binding of AGPN on swarming mobility protein of *P. aeruginosa*. BswR is a monomeric protein of *P. aeruginosa*, which acts as a transcription factor to synchronize the development of biofilm and accelerates the swarming motility (Wang et al. 2014). The docking result demonstrated that AGPN interacts with Pro60 and Val78 of BswR (Fig. 4d), which further indicates AGPN effectively moderate the signal transduction pathway of swarming motility of *P. aeruginosa* through a conformational alteration of BswR. We further checked the binding score of decoy molecules of AGPN with each protein of interest, excluding the hit list decoys having higher binding scores than the crystallographic structure extracted from Pub Chem (Powers et al. 2002). The decoy with best scoring geometry corresponds to the crystallographic ligand geometry within 2.0 Å RMSD, which was considered as native-like conformation (Supplementary Table S1) (Graves et al. 2005). Other reports showed that ligands could effectively bind to the proteins of interest such as Reserpine for RhlI, Neophytadiene for LasR chain A and Chain B, Thunbergol for LasI (Parai et al. 2018; Qais et al. 2019). In our study, these ligands were also considered to corroborate the findings of binding affinities of AGPN and proteins (RhlI, LasR, LasI, BswR), represented in supplementary Figure S2 (S2.1 to S2.5) and Supplementary Table S1. AGPN interacted

with the active site residues Ser98, Ser99, Phe 101 of RhlI protein with strong conventional hydrogen bond, carbon-hydrogen bond, and pi-alkyl bond, respectively, whereas the bond formed between Reserpine and nearby residue Val103 of the active site of RhlI is alkyl in nature. AGPN interacts with additional residues on the active sites of RhlI rather than Reserpine (Supplementary Figure S2.1), indicating strong affinity. In the case of lasI protein, Thunbergol tied up with only one active site residue Arg30 by conventional hydrogen bond, whereas AGPN forms two alkyl bonds and a conventional hydrogen bond with Phe105, Thr144, and Arg30, respectively (Supplementary Figure S2.2). Furthermore, another compound, namely Neophytadiene interacts with Chain A and Chain B of LasR through the active site residues Pro85 and Phe87 by making chemical bonds. On the other side, the same residues with an additional residue Leu8 interact with AGPN by alkyl bonds (Supplementary Figures S2.3 and S2.4). The strong binding affinity of AGPN towards the active sites of these proteins might be due to the structural topology of AGPN itself. Under the purview of the chemical structure of AGPN, it could be stated that the >C=O group of AGPN acts as hydrogen bond acceptor, whereas –NH or the –COOH terminal of the amino acids of the proteins act as H-bond donor. Additionally, AGPN has pi-electron in its 14th position, which is favourable for alkyl bond formation. As a consequence, we can state that AGPN acts as a potent molecule controlling the biofilm formation by making stable complexes using non-covalent interactions with quorum sensing proteins of *P. aeruginosa*.

The Las and Rhl are two central operon systems involved in the QS pathway, which yield C12-HSL and C4-HSL, respectively and regulating a series of genes required for biofilm production along with the secretion of virulence factors (Medina et al. 2003; Mukherjee et al. 2017). After performing in silico analysis, the mRNA level of the QS gene *rhlI* of *P. aeruginosa* was estimated to evaluate the effect of AGPN at the genetic level. AGPN effectively down-regulates the mRNA production of one of the main regulators *lasR* and one downstream gene *rhlI*, leading to reduce the amount of C4-HSL quantity. As a result, additionally, C4-HSL is not sufficiently available to bind the RhlI protein regulating the biosynthesis of the elastase enzyme (Mukherjee et al. 2017). These results resembled between docking studies and a qRT-PCR study showing AGPN is effectively binding with LasR and RhlI protein and downregulating *lasR* and *rhlI* gene (Fig. 5a), respectively. These strongly suggest a well-framed correlation between theoretical and experimental outcomes. The findings by biochemical experiments and in silico studies could easily correlate with the FE-SEM results, in which AGPN and GEN significantly disrupted the biofilm formation of *P. aeruginosa*. This interpretation implies the efficiency of AGPN in inhibiting biofilm in combination with the sub-MIC dose of antibiotic against *P. aeruginosa*.

In the present study anti-biofilm activity of AGPN is evaluated and found to be very noteworthy. Besides, AGPN shows inhibition of virulence factors and down-regulation of the quorum-sensing gene, accompanied by a hostile effect in structural alterations of biofilm of *P. aeruginosa*. Our data suggest that AGPN can be considered as an antibiofilm compound against bacterial biofilm.

Acknowledgements This work is supported by a Project Grant (File Number: YSS/2015/001965) to DNROY from Science and Engineering Research Board (SERB), Department of Science and Technology (DST), Govt. of India. MM is thankful to the National Institute of Technology, Agartala, for providing Ph.D. fellowship. Authors appreciate the facility of Atomic Force Microscopy (AFM) at Central Research Facility (CRF), National Institute of Technology Agartala. AD is thankful to ICMR, Govt. of India, for providing postdoctoral research fellowship. Real-Time PCR experiment was performed at the School of Bioscience, Indian Institute of Technology Kharagpur, and Fluorescence Microscope and FE-SEM were conducted at Tripura University, Tripura.

Compliance with ethical standards

Conflict of interest The authors declared that they have no conflict of interest.

References

Abinaya M, Gayathri M (2019) Inhibition of biofilm formation, quorum sensing activity and molecular docking study of isolated 3,5,7-trihydroxyflavone from *Alstonia scholaris* leaf against *P. aeruginosa*. Bioorg Chem 87:291–301

Andersson DI, Nicoloff H, Hjort K (2019) Mechanisms and clinical relevance of bacterial heteroresistance. Nat Rev Microbiol 17(8):479–496

Banerjee M, Moulick S, Bhattacharya KK, Parai D, Chattopadhyay S, Mukherjee SK (2017) Attenuation of *Pseudomonas aeruginosa* quorum sensing, virulence and biofilm formation by extracts of *Andrographis paniculata*. Microb Pathog 113:85–93

Barsoumian AE, Mende K, Sanchez CJ, Beckius ML, Wenke JC, Murray CK, Akers KS (2015) Clinical infectious outcomes associated with biofilm-related bacterial infections: a retrospective chart review. BMC Infect Dis 15(1):223

Bjarnsholt T (2013) The role of bacterial biofilms in chronic infections. Apmis 121:1–58

Bottomley MJ, Muraglia E, Bazzo R, Carfì A (2007) Molecular insights into quorum sensing in the human pathogen *Pseudomonas aeruginosa* from the structure of the virulence regulator LasR bound to its autoinducer. J Biol Chem 282(18):13592–13600

Cepas V, López Y, Munoz E, Rolo D, Ardanuy C, Martí S, Xercavins M, Horcajada JP, Bosch J, Soto SM (2019) Relationship between biofilm formation and antimicrobial resistance in Gram-negative bacteria. Microb Drug Resist 25(1):72–79

Choudhury R, Majumder M, Roy DN, Basumallick S, Misra TK (2016) Phytotoxicity of Ag nanoparticles prepared by biogenic and chemical methods. Int Nano Lett 6(3):153–159

Combrouse T, Sadovskaya I, Faille C, Kol O, Guérardel Y, Midelet-Bourdin G (2013) Quantification of the extracellular matrix of the *Listeria monocytogenes* biofilms of different phylogenic lineages with optimization of culture conditions. J Appl Microbiol 114(4):1120–1131

Costa OY, Raaijmakers JM, Kuramae EE (2018) Microbial extracellular polymeric substances: ecological function and impact on soil aggregation. Front Microbiol 9:1636

Cragg GM, Newman DJ (2013) Natural products: a continuing source of novel drug leads. Biochim Biophys Acta (BBA) 1830(6):3670–3695

Das MC, Sandhu P, Gupta P, Rudrapaul P, De UC, Tribedi P, Akhter Y, Bhattacharjee S (2016) Attenuation of *Pseudomonas aeruginosa* biofilm formation by vitexin: a combinatorial study with azithromycin and gentamicin. Sci Rep 6:23347

Debnath B, Majumdar M, Bhowmik M, Bhowmik KL, Debnath A, Roy DN (2020) The effective adsorption of tetracycline onto zirconia nanoparticles synthesized by novel microbial green technology. J Environ Manag 261:110235

Diggle SP, Winzer K, Lazdunski A, Williams P, Cámara M (2002) Advancing the quorum in *Pseudomonas aeruginosa*: MvaT and the regulation of N-acylhomoserine lactone production and virulence gene expression. J Bacteriol 184(10):2576–2586

Donlan RM (2002) Biofilms: microbial life on surfaces. Emerg Infect Dis 8(9):881

Donlan RM, Costerton JW (2002) Biofilms: survival mechanisms of clinically relevant microorganisms. Clin Microbiol Rev 15(2):167–193

Dubey A, Marabotti A, Ramteke PW, Facchiano A (2016) Interaction of human chymase with ginkgolides, terpene trilactones of *Ginkgo biloba* investigated by molecular docking simulations. Biochem Biophys Res Commun 473(2):449–454

Dubey A, Dotolo S, Ramteke PW, Facchiano A, Marabotti A (2019) Searching for chymase inhibitors among chamomile compounds using a computational-based approach. Biomolecules 9(1):5

Eliopoulos G, Moellering R Jr (1996). In: Lorian V (ed) Antimicrobial combinations. Antibiotics in laboratory medicine. Williams & Wilkins Co., Baltimore

Gao M, Teplitski M, Robinson JB, Bauer WD (2003) Production of substances by *Medicago truncatula* that affect bacterial quorum sensing. Mol Plant Microbe Interact 16(9):827–834

Gasteiger J, Marsili M (1980) Iterative partial equalization of orbital electronegativity—a rapid access to atomic charges. Tetrahedron 36(22):3219–3228

Ghosh S, Roy K, Pal C (2019) Terpenoids against infectious diseases. In: Terpenoids against human diseases. CRC Press, Boca Raton, pp 187–208

Gould TA, Schweizer HP, Churchill ME (2004) Structure of the *Pseudomonas aeruginosa* acyl-homoserinelactone synthase LasI. Mol Microbiol 53(4):1135–1146

Graves AP, Brenk R, Shoichet BK (2005) Decoys for docking. J Med Chem 48(11):3714–3728

Gutierrez M, Choi MH, Tian B, Xu J, Rho JK, Kim MO, Cho Y-H, Yoon SC (2013) Simultaneous inhibition of rhamnolipid and polyhydroxyalkanoic acid synthesis and biofilm formation in *Pseudomonas aeruginosa* by 2-bromoalkanoic acids: effect of inhibitor alkyl-chain-length. PLoS ONE 8(9):e73986

Haque M, Sartelli M, McKimm J, Bakar MA (2018) Health care-associated infections—an overview. Infect Drug Resist 11:2321

Hu Y, Ulstrup J, Zhang J (2012) Bacterial biofilms investigated by atomic force microscopy and electrochemistry. DTU Chemistry, Kgs Lyngby

Jung Y-G, Choi J, Kim S-K, Lee J-H, Kwon S (2015) Embedded biofilm, a new biofilm model based on the embedded growth of bacteria. Appl Environ Microbiol 81(1):211–219

Kan A, Birnbaum DP, Praveschotinunt P, Joshi NS (2019) Congo Red fluorescence for rapid in situ characterization of synthetic curli systems. Appl Environ Microbiol 85(13):e00434–e00419

Kearns DB (2010) A field guide to bacterial swarming motility. Nat Rev Microbiol 8(9):634

Kessler E, Safrin M (1994) The propeptide of *Pseudomonas aeruginosa* elastase acts an elastase inhibitor. J Biol Chem 269(36):22726–22731

Kim S, Thiessen PA, Bolton EE, Chen J, Fu G, Gindulyte A, Han L, He J, He S, Shoemaker BA (2015) PubChem substance and compound databases. Nucleic Acids Res 44(D1):D1202–D1213

Kumar L, Chhibber S, Harjai K (2013) Zingerone inhibit biofilm formation and improve antibiofilm efficacy of ciprofloxacin against *Pseudomonas aeruginosa* PAO1. Fitoterapia 90:73–78

Lázár V, Martins A, Spohn R, Daruka L, Grézal G, Fekete G, Számel M, Jangir PK, Kintses B, Csörgő B (2018) Antibiotic-resistant bacteria show widespread collateral sensitivity to antimicrobial peptides. Nat Microbiol 3(6):718

Lee C, Lee S, Shin SG, Hwang S (2008) Real-time PCR determination of rRNA gene copy number: absolute and relative quantification assays with *Escherichia coli*. Appl Microbiol Biotechnol 78(2):371–376

Li H, Qin H, Wang W, Li G, Wu C, Song J (2006) Effect of andrographolide on QS regulating virulence factors production in *Pseudomonas aeruginosa*. China J Chin Mater Med 31(12):1015–1017

Liu J, Wang Z-T, Ge B-X (2008) Andrograpanin, isolated from *Andrographis paniculata*, exhibits anti-inflammatory property in lipopolysaccharide-induced macrophage cells through down-regulating the p38 MAPKs signaling pathways. Int Immunopharmacol 8(7):951–958

Lu L, Hume ME, Pillai SD (2005) Autoinducer-2-like activity on vegetable produce and its potential involvement in bacterial biofilm formation on tomatoes. Foodborne Pathog Dis 2(3):242–249

Ma L, Liu X, Liang H, Che Y, Chen C, Dai H, Yu K, Liu M, Ma L, Yang C-H (2012) Effects of 14-alpha-lipoyl andrographolide on quorum sensing in *Pseudomonas aeruginosa*. Antimicrob Agents Chemother 56(12):6088–6094

Maisuria VB, Lopez-de Los Santos Y, Tufenkji N, Déziel E (2016) Cranberry-derived proanthocyanidins impair virulence and inhibit quorum sensing of *Pseudomonas aeruginosa*. Sci Rep 6:30169

Majumdar M, Roy D (2019) Terpenoids: the biological key molecules. Taylor & Francis, Milton Park, pp 39–60

Majumdar M, Biswas SC, Choudhury R, Upadhyay P, Adhikary A, Roy DN, Misra TK (2019a) Synthesis of gold nanoparticles using *Citrus macroptera* fruit extract: anti-biofilm and anticancer activity. ChemistrySelect 4(19):5714–5723

Majumdar M, Misra TK, Roy DN (2019b) In vitro anti-biofilm activity of 14-deoxy-11,12-didehydroandrographolide from *Andrographis paniculata* against *Pseudomonas aeruginosa*. Braz J Microbiol 51(1):15–27

Majumdar M, Khan SA, Biswas SC, Roy DN, Panja AS, Misra TK (2020) In vitro and in silico investigation of anti-biofilm activity of *Citrus macroptera* fruit extract mediated silver nanoparticles. J Mol Liq 302:112586

Medina G, Juarez K, Díaz R, Soberón-Chávez G (2003) Transcriptional regulation of *Pseudomonas aeruginosa* rhlR, encoding a quorum-sensing regulatory protein. Microbiology 149(11):3073–3081

Moradali MF, Ghods S, Rehm BH (2017) *Pseudomonas aeruginosa* lifestyle: a paradigm for adaptation, survival, and persistence. Front Cell Infect Microbiol 7:39

Morris GM, Huey R, Lindstrom W, Sanner MF, Belew RK, Goodsell DS, Olson AJ (2009) AutoDock4 and AutoDockTools4: automated docking with selective receptor flexibility. J Comput Chem 30(16):2785–2791

Mukherjee S, Moustafa D, Smith CD, Goldberg JB, Bassler BL (2017) The RhlR quorum-sensing receptor controls *Pseudomonas aeruginosa* pathogenesis and biofilm development independently of its canonical homoserine lactone autoinducer. PLoS Pathog 13(7):e1006504

Mysinger MM, Carchia M, Irwin JJ, Shoichet BK (2012) Directory of useful decoys, enhanced (DUD-E): better ligands and decoys for better benchmarking. J Med Chem 55(14):6582–6594

Niranjan Reddy V, Malla Reddy S, Ravikanth V, Krishnaiah P, Venkateshwar Goud T, Rao T, Siva Ram T, Gonnade RG, Bhadbhade M, Venkateswarlu Y (2005) A new bis-andrographolide ether from *Andrographis paniculata* nees and evaluation of anti-HIV activity. Nat Prod Res 19(3):223–230

Olsson MH, Søndergaard CR, Rostkowski M, Jensen JH (2011) PROPKA3: consistent treatment of internal and surface residues in empirical pKa predictions. J Chem Theory Comput 7(2):525–537

Ooi JP, Kuroyanagi M, Sulaiman SF, Muhammad TST, Tan ML (2011) Andrographolide and 14-deoxy-11, 12-didehydroandrographolide inhibit cytochrome P450s in HepG2 hepatoma cells. Life Sci 88(9–10):447–454

Pamp SJ, Gjermansen M, Johansen HK, Tolker-Nielsen T (2008) Tolerance to the antimicrobial peptide colistin in *Pseudomonas aeruginosa* biofilms is linked to metabolically active cells, and depends on the pmr and mexAB-oprM genes. Mol Microbiol 68(1):223–240

Parai D, Banerjee M, Dey P, Chakraborty A, Islam E, Mukherjee SK (2018) Effect of reserpine on *Pseudomonas aeruginosa* quorum sensing mediated virulence factors and biofilm formation. Biofouling 34(3):320–334

Patel JB (2017) Performance standards for antimicrobial susceptibility testing. Clinical and Laboratory Standards Institute, Wayne

Pearson JP, Van Delden C, Iglewski BH (1999) Active efflux and diffusion are involved in transport of *Pseudomonas aeruginosa* cell-to-cell signals. J Bacteriol 181(4):1203–1210

Powers RA, Morandi F, Shoichet BK (2002) Structure-based discovery of a novel, non-covalent inhibitor of AmpC β-lactamase. Structure 10(7):1013–1023

Priester JH, Horst AM, Van De Werfhorst LC, Saleta JL, Mertes LA, Holden PA (2007) Enhanced visualization of microbial biofilms by staining and environmental scanning electron microscopy. J Microbiol Methods 68(3):577–587

Qais FA, Khan MS, Ahmad I (2019) Broad-spectrum quorum sensing and biofilm inhibition by green tea against Gram-negative pathogenic bacteria: deciphering the role of phytocompounds through molecular modelling. Microb Pathog 126:379–392

Repasky MP, Shelley M, Friesner RA (2007) Flexible ligand docking with Glide. Curr Protoc Bioinform 18(1):8 (**11-18.12. 36**)

Roy B, Bharali P, Konwar BK, Karak N (2013) Silver-embedded modified hyperbranched epoxy/clay nanocomposites as antibacterial materials. Bioresour Technol 127:175–180

Roy DN, Mandal S, Sen G, Mukhopadhyay S, Biswas T (2010) 14-Deoxyandrographolide desensitizes hepatocytes to tumour necrosis factor-alpha-induced apoptosis through calcium-dependent tumour necrosis factor receptor superfamily member 1A release via the NO/cGMP pathway. Brit J Pharmacol 160(7):1823–1843

Roy DN, Sen G, Chowdhury KD, Biswas T (2011) Combination therapy with andrographolide and D-penicillamine enhanced therapeutic advantage over monotherapy with D-penicillamine in attenuating fibrogenic response and cell death in the periportal zone of liver in rats during copper toxicosis. Toxicol Appl Pharmacol 250(1):54–68

Saini R, Saini S, Sharma S (2011) Biofilm: a dental microbial infection. J Nat Sci Biol Med 2(1):71

Schillaci D, Cusimano MG, Cunsolo V, Saletti R, Russo D, Vazzana M, Vitale M, Arizza V (2013) Immune mediators of sea-cucumber *Holothuria tubulosa* (Echinodermata) as source of novel antimicrobial and anti-staphylococcal biofilm agents. AMB Express 3(1):35

Shelley JC, Cholleti A, Frye LL, Greenwood JR, Timlin MR, Uchimaya M (2007) Epik: a software proGram for pK a prediction and protonation state generation for drug-like molecules. J Comput Aided Mol Des 21(12):681–691

Simoes M, Bennett RN, Rosa EA (2009) Understanding antimicrobial activities of phytochemicals against multidrug resistant bacteria and biofilms. Nat Prod Rep 26(6):746–757

Singha PK, Roy S, Dey S (2003) Antimicrobial activity of *Andrographis paniculata*. Fitoterapia 74(7–8):692–694

Soni KA, Lu L, Jesudhasan PR, Hume ME, Pillai SD (2008) Influence of autoinducer-2 (AI-2) and beef sample extracts on *E. coli* O157:H7 survival and geen expression of virulence gene yadK and hhA. J Food Sci 73(3):M135–M139

Soto SM (2013) Role of efflux pumps in the antibiotic resistance of bacteria embedded in a biofilm. Virulence 4(3):223–229

Toder D, Gambello M, Iglewski B (1991) *Pseudomonas aeruginosa* LasA: a second elastase under the transcriptional control of lasR. Mol Microbiol 5(8):2003–2010

Wallis C, Melnick JL, Longoria CJ (1981) Colorimetric method for rapid determination of bacteriuria. J Clin Microbiol 14(3):342–346

Wang C, Ye F, Kumar V, Gao Y-G, Zhang L-H (2014) BswR controls bacterial motility and biofilm formation in *Pseudomonas aeruginosa* through modulation of the small RNA rsmZ. Nucleic Acids Res 42(7):4563–4576

Watson WT, Minogue TD, Val DL, von Bodman SB, Churchill ME (2002) Structural basis and specificity of acyl-homoserine lactone signal production in bacterial quorum sensing. Mol Cell 9(3):685–694

Wu Y-Q, Shan H-W, Zhao X-Y, Yang X-Y (2011) Nosocomial infection caused by *Pseudomonas aeruginosa* in intensive care unit. Chin Crit Care Med 23(2):88–90

Affiliations

Moumita Majumdar[1] · Amit Dubey[2] · Ritobrata Goswami[3] · Tarun Kumar Misra[1] · Dijendra Nath Roy[4]

✉ Dijendra Nath Roy
dnr_20@hotmail.com

[1] Department of Chemistry, National Institute of Technology, Agartala, Tripura, India

[2] Department of Molecular Biology, National AIDS Research Institute, Pune, Maharashtra, India

[3] School of Bioscience, Indian Institute of Technology, Kharagpur, West Bengal, India

[4] Department of Bio Engineering, National Institute of Technology, Agartala, Tripura, India